PERGAMON Progress in Quantum Electronics 27 (2003) 417–450

Progress in Quantum Electronics

www.elsevier.com/locate/pquantelec

On superluminal tunneling

Günter Nimtz*

II. Physikalisches Insitut, der Universität zu Köln, Zülpicher Straße 77, 50937 Koln, Germany

Abstract

Photonic tunneling is currently of theoretical and applied interest. In a previous review, faster-than-light (i.e. *superluminal*) *photonic tunneling* was discussed (Progr. Quantum Electron. 21 (1997) 81). Recently, superluminal photonic pulse transmission and reflection have been measured at microwave and infrared frequencies. It seems clear that superluminal photonic and electronic devices will become a reality in the near future.

In the present report, we introduce new experimental and theoretical data on superluminal tunneling and reflection. Data of reflection by barriers have evidenced the nonlocal nature of tunneling. Asymmetric barriers have revealed a strange asymmetric reflection behavior in time.

The principle of causality is not violated by a superluminal speed even though the time duration between cause and effect can be shortened compared with a luminal interaction exchange. An empirical relationship independent of the barrier system is found for the photonic tunneling time. This relation seems to be universal for all kind of tunneling processes in the case of single opaque barriers. We show that the superluminal velocity can be applied to speed up photonic modulation and transmission as well as to improve microelectronic devices.

Contents

*Tel.: +49-221-470-3594; fax: +49-221-470-2980.
E-mail address: g.nimtz@uni-koeln.de (G. Nimtz).

0079-6727/03/$ - see front matter
doi:10.1016/S0079-6727(03)00057-0

1. Introduction

In this second report on tunneling I shall review fundamental physical properties still not accepted by all physicists and on new experiments confirming superluminal signal velocity in tunneling. Superluminal signal velocities are not violating the principle of causality: the effect follows the cause and the design of time machines is not possible. This is disappointing for science fiction admirers who would like to manipulate the past. However, superluminal signal velocity allows to speed up photonic and electronic devices.

Superluminal velocity is the most spectacular property of the tunneling process: a purely imaginary tunneling time and thus a faster-than-light (superluminal) barrier traversal velocity have been predicted and observed [1,2]. The classical evanescent modes represent the general wave mechanical tunneling process [1,3,4]. At the end of the 19th century Rayleigh considered the group velocity to correspond to the velocity of energy or of signal transmission in vacuum. Later this raised difficulties in the relativistic theory of dispersive media. The problem was resolved by Sommerfeld and Brillouin in the case of waves with real and complex wave numbers with finite real part [5]. However, it was not tackled for media with purely imaginary wave numbers as is the case in the tunneling process.

Many textbooks and review articles deny the possibility of superluminal energy and signal velocities, see for instance Refs. [6–10]. In a recently published textbook on *Relativity*, *Groups*, *Particles*, a chapter is devoted to signal velocities *faster than light* [8]. These authors conclude that superluminal group velocities may have been measured, but state that *the initial packet gets completely deformed and unsuitable for perfect signal transmission during the course of propagation due to the vastly differing phase velocities of its various frequency components.* The authors claim that a signal velocity can never exceed c the vacuum velocity of light. Allegedly this has been proved by Einstein studying the light propagation about a 100 years ago [11].

The above-cited statement about *vastly differing phase velocities...* is incorrect in the case of photonic tunneling since evanescent modes have purely imaginary wave numbers and do not experience a phase change [1,12–15]. The sophisticated property of the tunneling process, i.e. the lack of a phase shift inside a barrier, can result in a superluminal signal velocity as discussed in Refs. [1,6,16–20] for example. Fig. 1 shows a measured Gaussian pulse-like microwave signal, which traveled with a group velocity faster than c without being *completely deformed and unsuitable for perfect signal transmission.* The missing pulse reshaping as expected from the barrier dispersion relation, is due to the appropriate frequency band limitation of the signal.

Recently even negative group velocities v_g were measured at frequencies near the resonance of electronic transitions [21,22]. Again the signals did not experience a massive deformation. But in the case of tunneling the purely imaginary refractive index is in charge of the superluminal group velocity, whereas in the case of near-resonant interaction the real part of the refractive index is finite and negative. This essential property of near-resonant interaction is different from tunneling with its purely imaginary refractive index. In general wave number k and refractive index n are related by $k = nk_0$, where $k_0 = 2\pi v/c$ is the wave number in vacuum, n is the refractive index of the media in question, and v the frequency. In this article superluminal signal transmission and partial reflection by tunneling barriers are discussed. Such tunneling electromagnetic waves (in optics they are called evanescent modes) play an important role in microwave technology, in modern optics, in

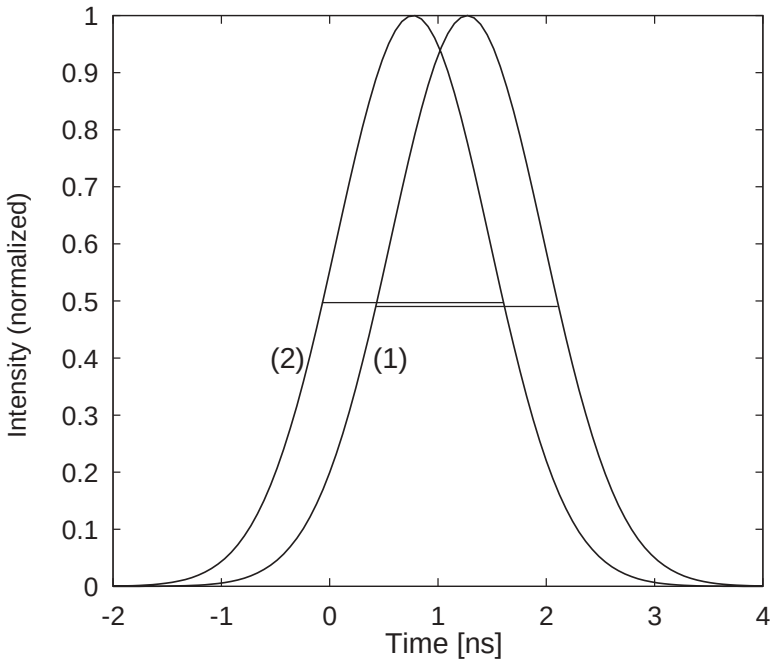

Fig. 1. Intensity vs. time of a microwave pulse (2) which has tunneled with superluminal velocity through a photonic barrier. (An undersized waveguide barrier of 114.2 mm length.) For comparison the tunneled digital signal is normalized with a pulse (1) which propagated through a normal waveguide of the same length. The tunneled signal (the half-width of the pulse) traveled at a speed of $4.7c$ and was measured 0.5 ns earlier than the guided signal which traveled with a velocity of $0.655c$ [16]. The tunneled microwave pulse contained about 10^9 photons.

tunneling spectroscopy and in optoelectronics. Due to the mathematical identity between the Helmholtz and the time-independent Schrödinger equations, photonic waves are useful for studying experimentally the quantum mechanical tunneling process. We do not report on superluminal effects found in Lorentz material media as it is studied in Ref. [23], for instance. Pioneering theoretical studies on superluminal solutions of the Maxwell equations were presented by Recami, see, for instance, Refs. [2,18,24]. Recami introduced the word *tachyon* for superluminal wave packets.

Three prominent photonic tunneling barriers are presented in Fig. 2. They are based on different physical mechanisms, but all barriers are characterized by a purely imaginary wave number for the field spreading. The undersized waveguide has no wave solution at frequencies below the cutoff frequency. The photonic lattice has forbidden frequency bands when for the wave transmission, destructive interference takes place. In the case of frustrated total internal reflection (FTIR) part of the reflected beam can tunnel through the forbidden gap to the second prism. This is the reason for the name FTIR. For an imaginary wave number the wave equation yields for the electric field $E(x)$ in the case of tunneling

$$E(x) = E_0 e^{i(\omega t - kx)} \Rightarrow E(x) = E_0 e^{i\omega t - \kappa x}, \tag{1}$$

where ω is the angular frequency, t the time, x the measured distance, k the wave number, and $\kappa = ik$ the *imaginary* wave number of the evanescent mode. The classical term *evanescent mode* is coined for a field fading away or tending to become imperceptible in consequence of its natural decay with distance.

Evanescent modes experience an attenuation of transmission due to reflection at barrier front faces. They do not experience a phase shift inside a barrier. This implies a zero time barrier traversal according to the phase-time relation

$$\tau = d\varphi/d\omega, \tag{2}$$

where τ, φ, ω are the phase-time, the phase, and the angular frequency, respectively. The observed short traversal time elapses at the front boundary of the barrier. In this

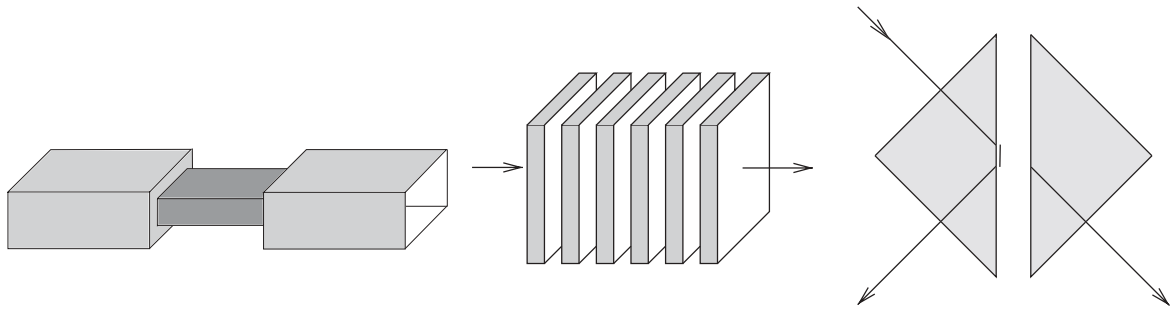

Fig. 2. Sketch of three prominent photonic barriers: (a) an undersized waveguide (the central part of the waveguide has a cross-section which is smaller than half the wavelength in both directions perpendicular to propagation); (b) a photonic lattice (periodic dielectric heterostructure); and (c) the FTIR of a double prism where total reflection takes place at the boundary from a denser to a rarer dielectric medium.

report the tunneling time is defined as the time a group or a pulse spends traversing a barrier. This time is measured from outside the barrier at the front to outside the barrier at the back. Replacing the barrier by an air distance of the same length represents a perfect calibration of the setup. The time measured corresponds to the group time delay, see Refs. [14,25–27], for example.

The traversal time caused by the front boundary is independent of barrier length [27]. Thus with increasing barrier length the group velocity increases at the same rate as the length. This phenomenon is often called Hartman effect [18,28] and has been shown first in a microwave experiment [28] and later confirmed with laser pulses [29].

In Fig. 3 a pulse (i.e. a wave packet) is sketched which represents a digital signal. The front of the envelope is very smooth corresponding to a narrow frequency bandwidth Δv. The radiated frequency occupies the frequency band

$$\Delta v = v(\max) - v(\min) \tag{3}$$

$$= 2v_{\mathrm{mod}}(\max) \tag{4}$$

with

$$v(\max) = v_{\mathrm{c}} + v_{\mathrm{mod}}(\max) \tag{5}$$

$$v(\min) = v_{\mathrm{c}} - v_{\mathrm{mod}}(\max), \tag{6}$$

where v_{c} and v_{mod} are the carrier frequency and the modulation frequency, respectively [30].

In the case of superluminal tunneling a narrow frequency band is choosen with respect to the barrier in question in such a way that the pulse contains essentially evanescent frequency components only. Such an evanescent pulse can travel in zero time through opaque barriers, which in turn results in an infinite velocity in the phase-time approach neglecting the phase shift at the barrier front. This strange result has been conjectured by Hartman [1,27,31]. There are many theoretical

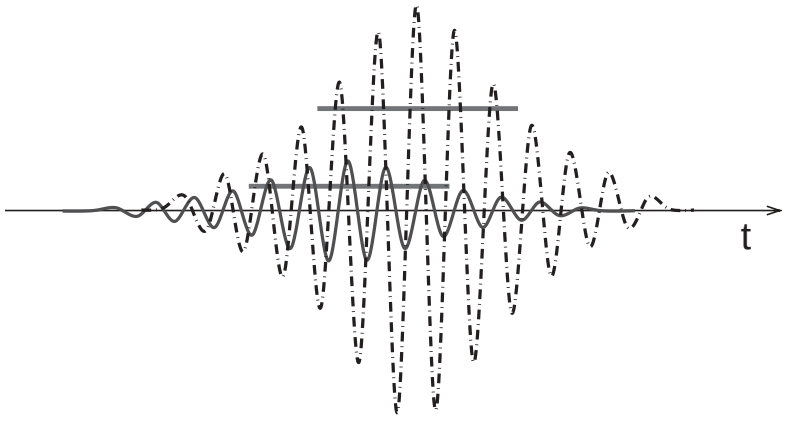

Fig. 3. Sketch of two wave packets (i.e. pulses), amplitude vs. time. The larger packet traveled slower than the attenuated one. The horizontal bars indicate the half-width of the packets which represent the information independent of the packets attenuation. The figure illustrates the gradual beginning of the packets [5]. The forward tail of the smooth envelope may be described by the relation $[1 - \exp(-t/a)][\sin(\omega t)]$ for instance, where a is a time constant.

approaches published in order to get a finite tunneling time [32]. However, in the review on *The quantum mechanical tunneling time problem—revisited* by Collins et al. [33], the following statement has been made: *the phase-time result originally obtained by Wigner and by Hartman is the best expression to use for a wide parameter range of barriers, energies and wave packets.* The experimental results of photonic tunneling have confirmed this statement and made all the efforts to find a finite tunneling time inside a barrier absurd.

Einstein causality prohibits superluminal signal velocity in vacuum and in media with a finite real component of the refractive index. (The general principle of causality prohibits only the exchange of cause and effect [16,17,34].) Einstein causality does not hold for media characterized by a purely imaginary refractive index where the phase shift is zero as in the case of evanescent mode propagation and quantum mechanical tunneling. A zero phase shift corresponds to an instantaneous field spreading, i.e. it represents an action at a distance. However, as explained in Chapter 5 a signal velocity faster than c still does not allow an exchange of cause and effect.

In order to avoid signal reshaping due to the dispersion of media, the signal has to be properly frequency band limited. Frequency band limitation and finite time duration are found for all physical signals and have been discussed and analyzed in Refs. [5,25,30], for instance. The impossibility of a hypothetically unlimited frequency band of signals has been explained by quantum mechanical arguments [16,17]. Such a signal has an infinite energy.

Actually, signals of limited frequency band and limited temporal width have been transmitted in the multiplex telephony for more than a 100 years. A historical picture of multiplex telephony is shown in Fig. 4. The continuous signals of the five telephone connections were periodically sampled and sent across one transmission line. Thus the continuous signals now are limited in time. According to Fourier transform theory a signal can either be limited in the frequency domain or in the time domain. The theory for signals which are limited in both frequency bandwidth and time duration is built upon the sampling theorem, which has been introduced by

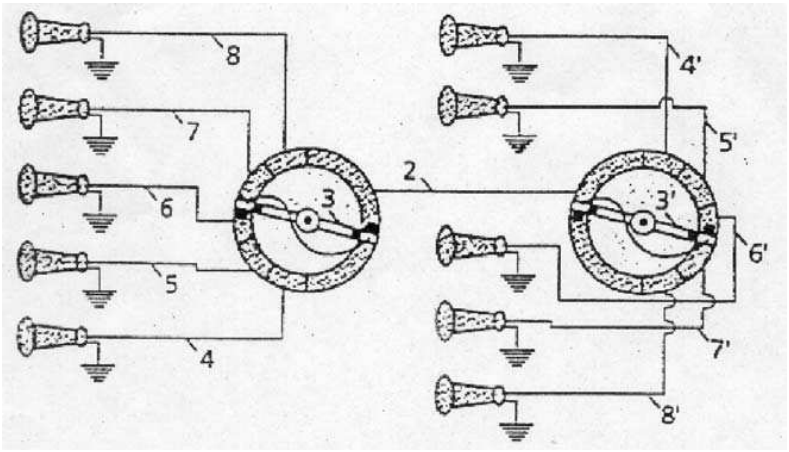

Fig. 4. Historical picture of a multiplex transmission system Ref. [35].

Shannon around 50 years ago [36]. More details about signal properties are presented in the following chapter on signals.

I wish to mention some special properties of evanescent modes. Evanescent modes are solutions of the classical Maxwell equations. However, they display some nonclassical properties, as for instance:

(1) Evanescent modes are represented by nonlocal fields as was predicted and later shown by transmission and by partial reflection experiments [1,27,37]. The nonlocal behavior follows from the purely imaginary wave number and from the experimental fact that tunneling and reflection times are equal, and they are independent of barrier length [37–39].
(2) Evanescent modes can be described by virtual photons [40].
(3) Evanescent modes (like tunneling particles in quantum mechanics, see Ref. [13] for instance) cannot be measured, they can be detected only behind a barrier [12,38]. Inside a barrier their energy is negative as the permeability is negative $\varepsilon = \kappa^2 < 0$ [12]. Detectors measure only positive energy quanta $\hbar\omega$ and not field strengths. The latter property is assumed in classical physics.
(4) Evanescent modes violate the theory of special relativity as $v_s \to \infty$ holds.

Obviously, evanescent modes are not fully describable by the Maxwell equations and by the theory of special relativity. Quantum mechanics has to be taken into consideration: evanescent modes are described by the quantum mechanical tunneling process. Some new photonic tunneling experiments and calculations are revisited in the following chapters. The essential properties of a physical signal as well as the existence of a universal tunneling time are introduced. Incidentally, it will be shown that superluminal signal velocity does not violate the principle of causality.

In 1992 Enders and Nimtz demonstrated for the first time that photonic tunneling may proceed with superluminal velocity. The experiments were carried out with microwaves in undersized waveguides [41]. At that time any application of superluminal tunneling was not expected in spite of the popular semiconductor tunneling diode. A decade later we are going to present experimental examples of overwhelming evidence for the possibility of superluminal signal velocity. In the final sections some potential applications of superluminal tunneling in photonics and in electronics are presented.

2. On some photonic tunneling experiments

In this chapter new experimental data and two simple experimental methods for measuring the photonic tunneling time in transmission and reflection are introduced. The methods are appropriate for all barrier structures. Other setups are presented in the previous article [1].

Incidentally, the effective barrier length and thus the traversal velocity can be significantly increased by resonant barrier structures. The transmission minimum is not decreased but the evanescent frequency bandwidth becomes narrower. An

example of a resonant tunneling structure is sketched in Fig. 5. Resonant tunneling structures with forbidden frequency bands are advantageous to speed up signals with a narrow frequency bandwidth [1,42–44]. Fig. 5 displays a resonant barrier built of two photonic lattices. The dispersion relations of the transmission coefficients and of the group velocity of this dielectric quarter wavelength heterostructure are displayed in Fig. 6. For narrow frequency band limited signals there is no significant dispersion effect if the carrier frequency is placed in the center of a forbidden frequency gap. Signals in communication systems have a typical bandwidth of $\Delta\nu/\nu = 10^{-4}$ only.

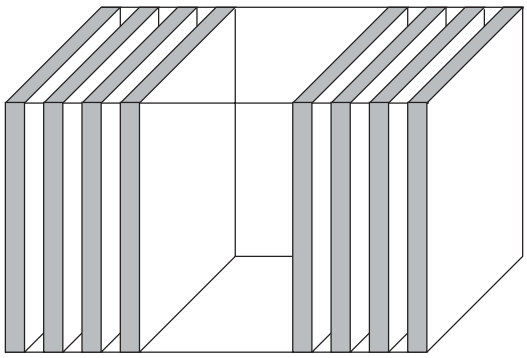

Fig. 5. An example of a resonant electromagnetic tunneling structure with evanescent mode solutions (forbidden frequency bands) at microwave frequencies (see Fig. 6). Two periodic quarter wavelength heterostructures of perspex and air are separated by an air distance of 189 mm forming a resonant cavity with an overall length of 280 mm. The perspex slabs are 5 mm thick and separated by an air distance of 8.5 mm.

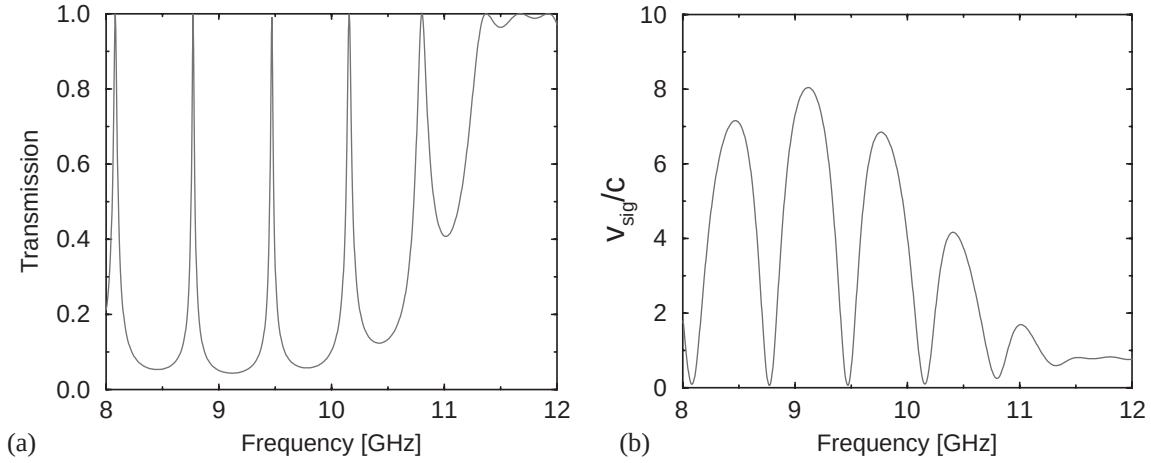

Fig. 6. The graph (a) shows the dispersion relation for the resonant heterostructure of Fig. 5 vs. frequency. The transmission dispersion of the periodic heterostructure displays forbidden gaps separated by resonant peaks. The forbidden frequency gaps correspond to the tunneling regime, for details see Ref. [1]. The evanescent regime is characterized by a strong attenuation due to reflection. In (b) the group velocity v_{sig} in units of c is displayed for the same resonant heterostructure vs. frequency.

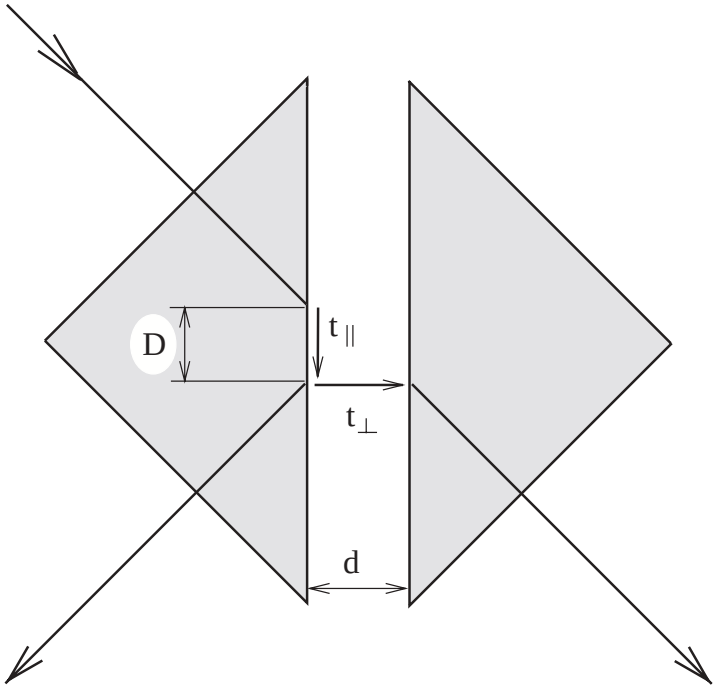

Fig. 7. Geometry of the incident, the reflected, the transmitted beam, and the tunneling time of the double-prism experiment. The tunneling time consists of two components. $t_{\|}$ for the Goos–Hänchen shift D parallel to the prism's surface and $t_{\perp}$ for crossing the gap in the direction perpendicular to the two surfaces. The total reflection presented here is often called FTIR because of the reflection loss due to the tunneling process.

The three barriers introduced in Fig. 2 have different dispersion relations. A simple one describes the FTIR of a double prism displayed in Fig. 7.[1] In this case of FTIR the transmitted electric field E_t and the imaginary wave number κ are defined by the relations [4]:

$$E_t = E_0 e^{(i\omega t - \kappa x)}, \tag{7}$$

$$\kappa = \left[\frac{\omega^2}{c^2}\left(\left(\frac{n_1}{n_2}\right)^2 \sin^2\theta - 1\right)\right]^{1/2}, \tag{8}$$

where θ is the angle of the incident beam, E_0 the electric field at the barrier entrance, x the barrier length (i.e. the gap), n_1 and n_2 are the refractive indices, and $(n_1/n_2)\sin\theta > 1$. The transmission as a function of air gap of a double prism was measured with microwaves and is shown in Fig. 8. The displayed transmission data at two frequencies are in agreement with Eqs. (7) and (8).

In studies of FTIR, superluminal tunneling velocities have been measured for the propagation in the air gap between the two prisms. The experiments were performed with pulses in the THz-frequency regime by Balcou and Dutriaux [45] and Carey

[1] In the previous review article [1] on photonic tunneling the beam paths are not correctly drawn as also in almost all published papers and text books (see for instance Ref. [4]). Also the Goos–Hänchen shift was not considered properly.

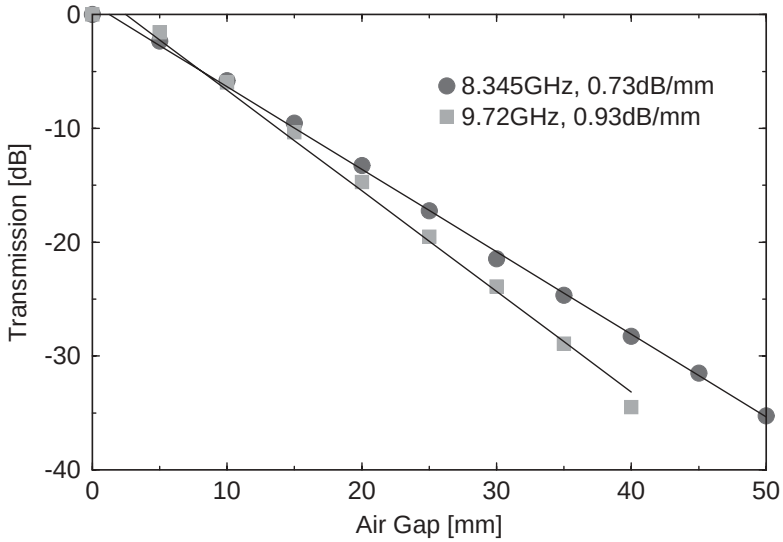

Fig. 8. Transmission (log-scale) vs. air gap measured at two frequencies [39]. The data follow the theoretical relations of Eqs. (7) and (8). $n_1 = 1.6$, $n_2 = 1$, and $\theta = 45°$. The critical angle of total reflection is $\theta_c = 38.5°$. The two prisms are cut from a 400 mm × 400 mm × 400 mm perspex cube.

et al. [46], and with pulses in the GHz-regime by Haibel et al. [39]. Both energy and group velocities of the measured pulses are greater than c. Detectors measure the arrival of energy in quanta of $\hbar\omega$. In the symmetrical arrangement of the double prisms experiment it is easily demonstrated that the reflected and the tunneled pulse leave the prisms at the same time. This result shows that the pulse spent no time for traversing the gap [39].

The tunneling time in the case of FTIR has been revisited recently [39,47]. There is a theoretical shortcoming in describing the time behavior of FTIR which is based on the approach with plane waves. This approach holds for an unlimited beam diameter, but is not mimicking properly the experimental procedure with limited beam diameters [39,48]. The latter is a condition sine qua non in all the experiments.

The following three experiments demonstrate superluminal signal velocity in tunneling photonic barriers. The signals are represented by pulses as used in digital communication systems [12,16,49]; two experiments were carried out at microwave and one at infrared frequencies. The data are displayed in Figs. 1, 9 and 10.

Two experimental setups to demonstrate superluminal signal velocity in transmission and in reflection are shown in Figs. 11 and 12. The arrival time was measured in air where group, energy, and signal velocities are equal to c [5,50].[2] Amplitude modulated microwaves with a frequency of 9.15 GHz ($\lambda = 3.28$ cm) are generated with an HP 8341B synthesized sweeper (10 MHz–20 GHz). A parabolic antenna transmitted parallel beams. The transmitted signal has been received by another parabolic antenna, rectified by a diode (HP 8472A (NEG)) and displayed on an oscilloscope (HP 54825A).

[2] Actually, as illustrated in Fig. 3 a signal does not depend on its magnitude.

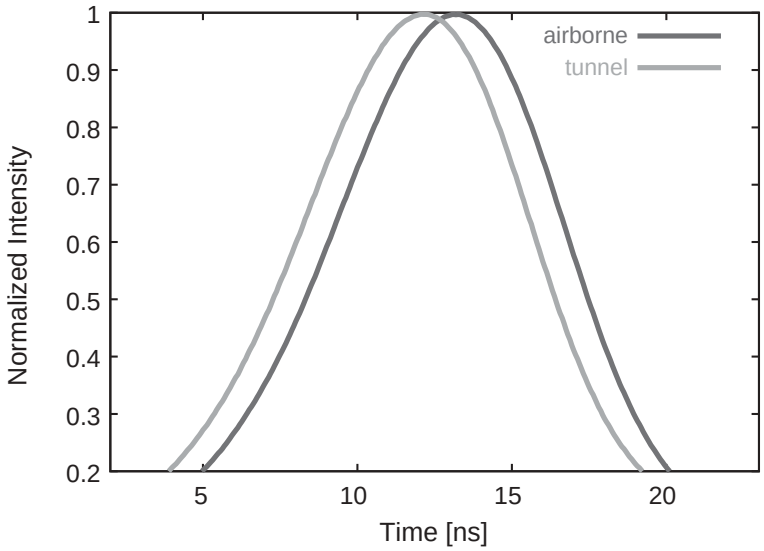

Fig. 9. Measured traversal time of two pulses. The faster one has tunneled in the forbidden frequency gap of the photonic barrier of length 280 mm. The pulse magnitudes are normalized. The tunneled signal (the half-width of the pulse, representing one bit) traversed the barrier 900 ps faster than the airborne pulse. The corresponding velocity of the tunneled pulse was $8c$ and the carrier frequency was 9.15 GHz. The barrier data are displayed in Figs. 5 and 6.

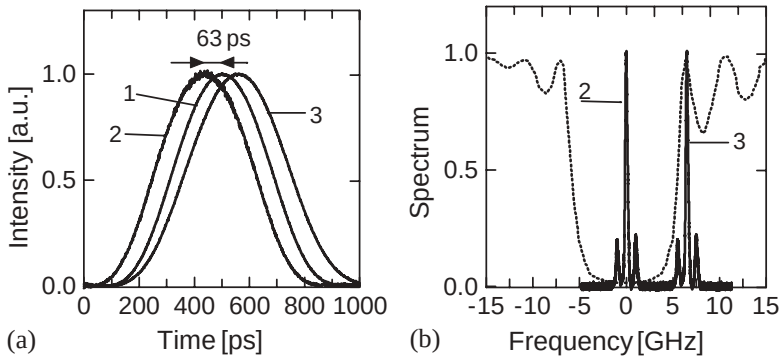

Fig. 10. Measured propagation time of three digital signals [49]. (a) Pulse trace 1 was recorded in vacuum. Pulse 2 traversed a photonic lattice in the center of the frequency band gap (see part (b) of the figure) at the speed of $2c$, and pulse 3 was recorded for the pulse traveling through the fiber outside the forbidden band gap. The photonic lattice was a periodic dielectric heterostructure fiber.

The performed measurements are asymptotic. There is no coupling between the generation process, the detection process and the photonic barrier. In addition, the experiment is not stationary and the pulse is measured in the dispersion free vacuum. The experimental situation is the same as that performed in the Hong-Ou-Mandel interferometer, in which the measurement is also asymptotic and yields the group velocity and the energy velocity at the same time using a large ensemble of single photons [51,52].

The propagation time of a pulse displayed in Fig. 9 was measured across the air distance between transmitter and receiver and across the same distance but partially filled with the barrier of $x = 280$ mm length. The barrier structure is formed

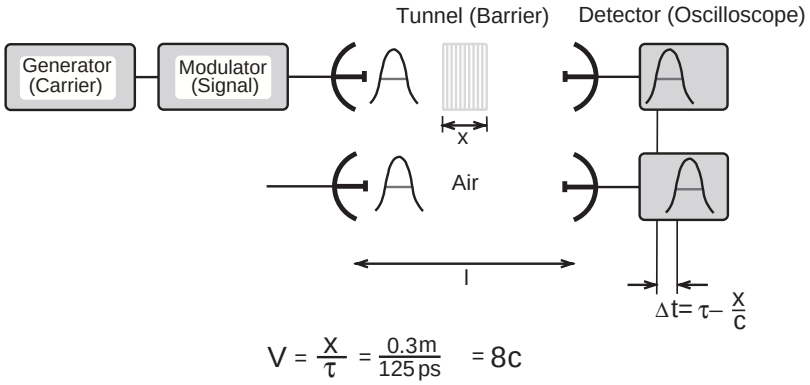

Fig. 11. Experimental setup for the periodic dielectric quarter wavelength heterostructure to measure the group velocity, i.e. the pulse velocity. An example is shown in Fig. 9.

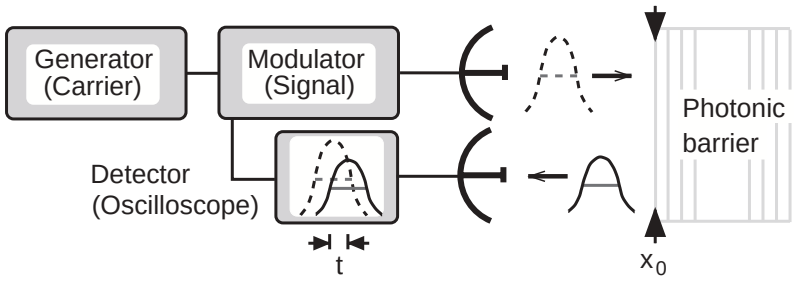

Fig. 12. Experimental setup to measure the partial reflection by a photonic lattice.

by quarter wavelength slabs of perspex and is introduced and analyzed in Figs. 5 and 6.

Comparing the two traveling times we see that the tunneled pulse and its half-width arrived at the detector about $\Delta t = 900$ ps earlier than that pulse which traveled the same distance through air

$$\Delta t = \frac{x}{v_g} - \frac{x}{c}. \tag{9}$$

The result corresponds to a signal velocity v_g of the tunneled pulse of $8c$,

$$v_g = \frac{x}{\Delta t + x/c}. \tag{10}$$

An example of superluminal velocity of an infrared signal traveling along a fiber is displayed in Fig. 10. Tunneling resulted in a signal velocity of $2c$. Outside the forbidden frequency gap the refractive index of 1.4 of the fiber reduces the velocity as shown by pulse 3 in Fig. 10. Details of the experiment are given in Chapter 7 on Photonic Applications, Section 7.1(a).

So far we have discussed transmission experiments only. An experimental setup for measuring the partial reflection by photonic barriers at microwave frequencies is presented in Fig. 12. The procedure of varying the barrier length in order to measure the dependence of reflection time on barrier length is sketched in Fig. 13.

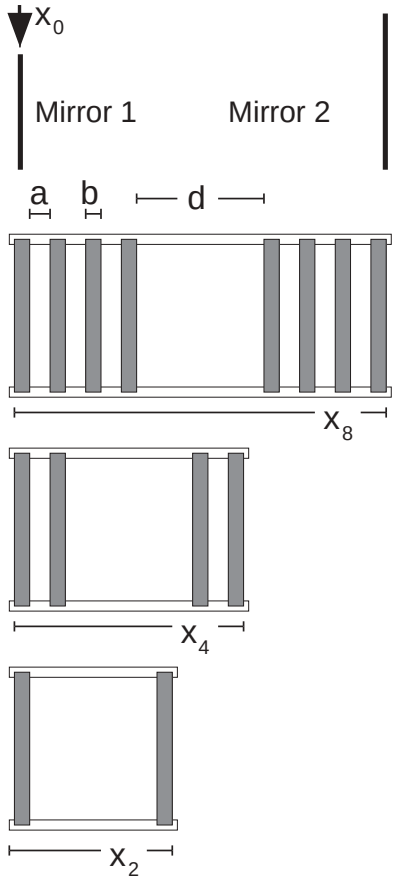

Fig. 13. Experimental procedure to measure partial reflection depending on a photonic resonant lattice structure. Here a and b are the layer thicknesses of air and of perspex, and d is the distance between the two photonic lattices. The barrier lengths are x_8, x_4, x_2.

3. Signals

A signal transmits information. We repeat briefly some essential properties of signals. For instance, a signal may be an astrophysical X-ray outburst. The centerfrequency of the outburst photons gives information on the temperature and the signal half-width on the total energy involved in the event. A signal may be a transmitted word, which informs the receiver. Both examples are described by wave packets of limited frequency bandwidth and of finite time duration. The envelope of a wave packet is traveling at no more than the speed of light in vacuum. Every part of the envelope is traveling at the signal velocity. The information has been received only after the complete envelope is measured. The front and the end are continuous rather than discontinuous events in time. A discontinuous signal represents an ideal, i.e. mathematical signal [5], which requires an infinite frequency bandwidth.

Examples of signals are displayed in Figs. 1, 10, 14 and 17. Signals are either amplitude modulated (AM) with voltage V given by

$$V = V_0(\cos \omega_c t)(1 + a_m \cos \omega_{mod} t), \tag{11}$$

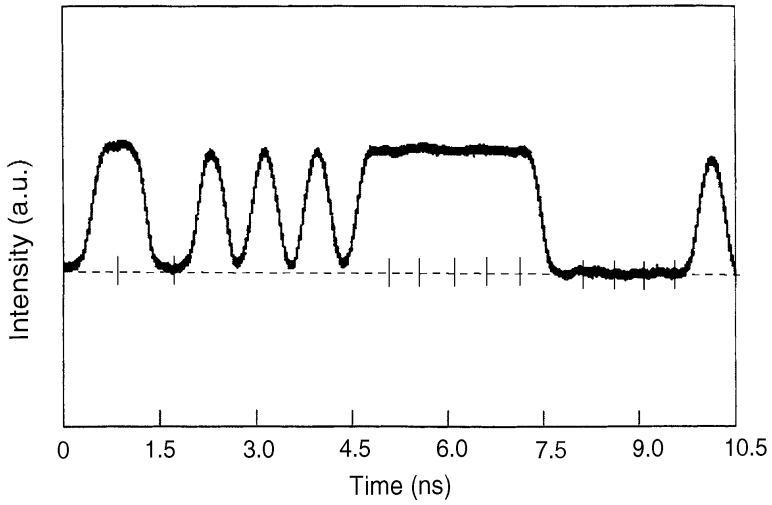

Fig. 14. Signals: measured signal in arbitrary units. The half-width in units of 0.2 ns corresponds to the number of bits. From left to right: 1, 1, 0, 0, 1, 0, 1, 0, 1, 0, 1, 1, 1, 1, 1, … . The infrared carrier frequency of the signal is 2×10^{14} Hz (wavelength 1.5 μm). The frequency bandwidth of the signal is about 2×10^{10} Hz corresponding to a relative frequency bandwidth of 10^{-4} [53].

or frequency modulated (FM) given by

$$V = V_0 \cos[\omega_c(1 + a_m \cos \omega_{mod} t)], \tag{12}$$

where ω_c and ω_{mod} are the carrier angular frequency and the modulation angular frequency, respectively. a_m presents the modulation amplitude. Definitions of the frequency bandwidth, of the time duration, and of the bandwidth–time interval product are introduced and explained in Refs. [25,30,54], for example.

As mentioned above the Fourier transform yields for frequency band limited signals an unlimited time extension and hence a noncausal behavior. The signal would exist before it is switched on. However, such noncausal time components have never been detected. In the case of an unlimited frequency band the wave packet may be presented by an analytic function, in which case the information contained in the forward tail of the packet determines the whole packet [55]. This is mathematically correct but not relevant for signals from the physical point of view.

As illustrated in Fig. 4 engineers have transmitted signals with the multiplex technology already a 100 years ago. In the historic picture of a multiplex transmission system five signals are transmitted over one guide and they are both frequency band and time duration limited. In this example the frequency bandwidth has been 2 kHz and the time length about 0.3 ms. Theoretical investigations Shannon's and many others provided the theory for the sampling technique. The Fourier transform of such a multiplex technique yields a noncausal behavior. This indicates that noncausal time components expected from Fourier transform are not detectable as they are not physical [16,17].

A signal is thought to cause a defined effect. Basically phonons, photons and electrons are exploited to mediate interaction or to transmit bits, words or any desired signal to induce required effects. The signal front or the discontinuous

beginning of a signal is a mathematical quantity defined only in the case of an infinite frequency spectrum. A physical transmitter produces signals with finite spectra only. In Ref. [56] it is claimed that *frequency band limitation is of course a technical and not a fundamental limitation*. This statement is not correct since frequency band limitation is a fundamental physical limitation as has been discussed in Refs. [12,14,36,57]. The front of a signal does not have a physical meaning. Only the complete envelope as defined and discussed in Ref. [25], for instance, provides the appropriate signal description.

Examples of digital signals are displayed in Figs. 1, 10 and 14. In general a signal is presented by wave packets with a mean momentum $p_0 = \hbar k_0$, corresponding to a carrier frequency v_0, and to frequency and amplitude modulation of half-width Δp. This becomes obvious in modern digital optoelectronic communication systems where measuring the half-width of a signal gives the number of digits, as displayed in Fig. 14. This modern signal reminds us of the historical Morse alphabet.

The definitions of velocities, which are presented extensively elsewhere, e.g. in Refs. [1,25,30,50], are

$$\text{Phase velocity } v_\varphi = \omega/k, \tag{13}$$

$$\text{Group velocity } v_g = d\omega/dk, \tag{14}$$

$$\text{Signal velocity } (\textit{in vacuum}) \; v_s \equiv v_g, \tag{15}$$

where ω and k are the angular frequency and the wave number, respectively.

For the problem of signal transmission the following terms are used to describe the delay of the various parts of a signal envelope. The delay times have been analyzed, for instance, in the textbook on Fourier Transform by Papoulis [25]

$$\text{Phase-time delay } t_\varphi(\omega) = \varphi(\omega)/\omega, \tag{16}$$

$$\text{Group time delay } t_g(\omega) = \tau = d\varphi(\omega)/d\omega, \tag{17}$$

$$\text{Front time delay } t_{fr}(\omega) = \lim_{\omega \to \infty} \varphi(\omega)/\omega, \tag{18}$$

where φ is the phase of the wave. The frequency band $A(\omega)$, the phase angle $\varphi(\omega)$, and the delay times are illustrated in Fig. 15. If $\varphi(\omega)$ does not tend to a straight line as ω tends to infinity, then the term *front time delay* of Eq. (18) has no meaning [25]. This behavior takes place in the case of frequency band limited signals in any medium, moreover in the case of tunneling, where the wave number is imaginary and thus the angle $\varphi = kx$ does not depend on the length x. (Obviously tunneling represents a nonlocal process.) If the signal is frequency band limited, a distortion of the envelope due to the dispersion by the medium can be avoided. In this case the delay of the signal envelope is assumed to equal the delay of the center of gravity [25].

The classical forerunners propagating with c [1,50] do not exist in the case of a tunneling signal containing evanescent modes only, since for all signal components $t_g = 0$ holds and t_{fr} is not defined (Eqs. (16) and (18)).

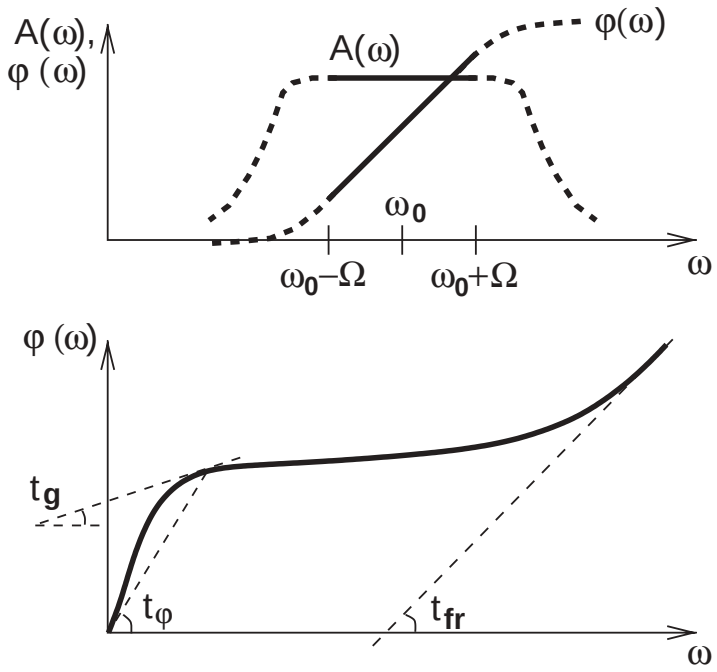

Fig. 15. A sketch of the spectrum of a frequency-band-limited signal with amplitude $A(\omega)$ vs. angular frequency ω, of phase angle $\varphi(\omega)$, and of various delay times as defined in Eqs. (16)–(18), see Ref. [25]. $\omega_0 \pm \Omega$ is the frequency bandwidth around the center frequency ω_0.

4. Superluminal signals

Since the Helmholtz and the time-independent Schrödinger equations are mathematically analogous, the three kinds of photonic barriers displayed in Fig. 2 can be used to model the one-dimensional process of wave mechanical tunneling [3,4].

4.1. Double-prisms

Superluminal tunneling data obtained with the historical double-prism experiment will be presented in the following [39]. This sophisticated experiment elucidates the time behavior of the tunneling process [47]. Fig. 7 indicates that for an angle of incidence larger than the angle of total reflection, the barrier transmission time of the double-prism, or what we call the tunneling time, can be split into two components

$$t_{\text{tunnel}} = t_{\parallel} + t_{\perp}, \tag{19}$$

one along the surface due to the Goos–Hänchen shift D, and another part perpendicular to the surface [39,47]. The measured tunneling time t_{tunnel} represents the group time delay which results in the group or signal velocity.

The first component of t_{tunnel} is related to a nonevanescent wave characterized by the real wave number

$$k_{\parallel} \coloneqq k_0 n_1 \sin\theta_i, \tag{20}$$

while the second one

$$k_\perp := ik_0\sqrt{n_1^2 \sin^2\theta_i - 1} \tag{21}$$

is related to the evanescent mode traversing the gap between the two prisms, where $k_0 = 2\pi/\lambda_0$ holds, λ_0 is the corresponding vacuum wavelength, and n_1 the refractive index of both prisms. For the refractive index of the gap is assumed $n_2 = 1$. Details of the experiment are given in Ref. [39].

In the symmetrical design of the microwave experiment displayed in Fig. 7, it was observed that the reflected and tunneled signal leave the left and the right prisms at the same time. This exciting result makes evident that for the tunneling time component $t_\perp = 0$ holds. The result is in agreement with the observations on other photonic tunneling structures: the small measured tunneling time originates from the barrier entrance boundary but no time is spent inside the barrier [1,39,47]. There are several other studies reporting on the tunneling time of FTIR at the double barrier, see Refs. [45,46] for instance. Other time-dependent FTIR investigations are handicapped by poor precision of the experimental analysis due to the short wavelength in the optical frequency regime or by using beams which are not parallel due to the use of horn antennas or by measuring very near the critical angle of total reflection. Thus beam components may have been reflected below the critical angle.

4.2. Photonic lattices

There are many studies on tunneling by photonic lattice structures. Here we mention only two outstanding experimental investigations. A couple of months after the discovery of superluminal tunneling of microwave signals [41], a study on superluminal group and energy velocities of single optical photons (twins) in tunneling a barrier was published by Steinberg et al. [51]. The group velocity v_g of the investigated black box (here the tunneling barrier) has been determined by averaging the tunneling time of many millions of photons. This procedure of averaging a huge ensemble of photons was compulsory as the spontaneous emission of the twins had a time jitter of 20 fs, whereas the average tunneling time was only ≈ 2 fs. This procedure is equivalent to sending signals each containing millions of photons, as was done in the microwave experiments. Incidentally, Steinberg et al. [52] used the same experimental setup to measure the subluminal group velocity of a sample of bulk glass in the black box. In this sophisticated experimental setup always the group velocity is measured and the procedure implies that the measured group velocity equals the signal velocity.

An FM experiment was carried out by Aichmann et al. [58]. They modulated Mozart's 40th symphony on a microwave carrier of 8.7 GHz and tunneled it in the frequency band gap of a photonic lattice. The signal with a bandwidth of 2 kHz traversed the barrier of 114.2 mm length at a speed of $4.7c$. The modulation of the signal and thus the music traveled at this superluminal velocity. The time gain compared with the traveling time of the airborne signal was 300 ps.

5. Does a superluminal signal violate the principle of causality?

According to many textbooks and review articles, a superluminal signal velocity violates Einstein causality, implying that cause and effect can be interchanged and time machines known from science fiction can be constructed [7–9]. On the other hand it can be shown for frequency band *unlimited groups* that the front travels always at a velocity $\leqslant c$, and only the peak of the signal has traveled with a superluminal velocity. Such calculations were carried out by several authors, for example Refs. [59–61]. A typical result of such calculations is presented in Fig. 16. The tunneled pulse is reshaped and its front has propagated at luminal velocity. The tunneled front does not travel faster than the airborne pulse. Only the peak has traveled with a velocity faster than c. This behavior is different from frequency band limited signals composed of evanescent frequency components only. Examples are presented in Figs. 1, 3, 10 and 14. In this case the pulses have gradually formed a front tail as sketched in Fig. 3. A pulse reshaping did not happen and the envelope and thus the signal traveled at a superluminal velocity.

Recently Winful calculated superluminal transport of pulses with narrow frequency bandwidth [61]. He believes that a superluminal signal velocity would violate the principle of causality and provided a theory to resolve the *mystery of apparent superluminality* in a strange and incorrect way. He claimed that the incoming pulse is not related to the outcoming pulse and he did not consider the nonlocal property of the tunneling process.

Superluminal signaling becomes especially obvious in the case of FM signals. Fig. 17 displays an FM signal as described by Eq. (12). The time duration between

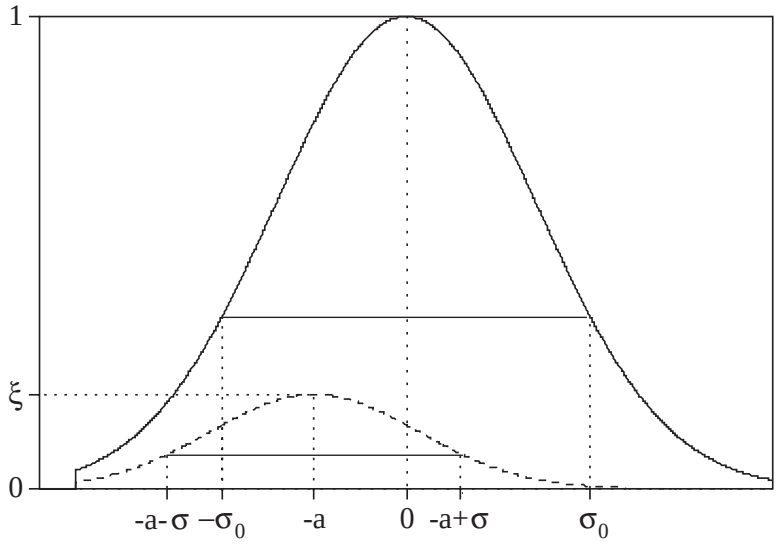

Fig. 16. Comparison of calculated intensity vs. time of an airborne signal (solid line) and a tunneled signal (dotted line) [59]. Both signals have a sharp step at their front and thus an *infinite* frequency bandwidth. The tunneled signal is reshaped, attenuated, and its maximum has traveled at superluminal velocity. Both fronts have traversed the same distance with speed c, ξ is the maximum of the tunneled pulse, a is the shift of the maximum, σ is the variance of the tunneled signal, and σ_0 is the variance of the airborne signal [59].

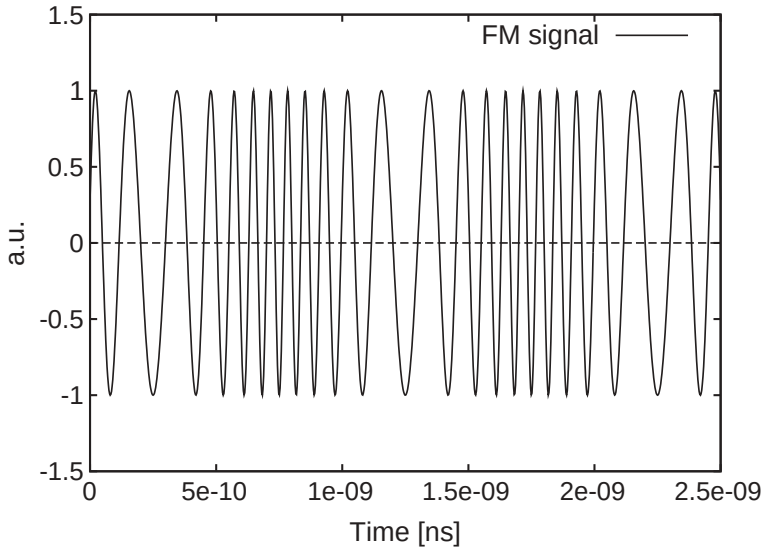

Fig. 17. A numerical example of an FM signal described by Eq. (12) where $\nu_c = 10$ GHz and $\nu_{mod} = 1$ GHz.

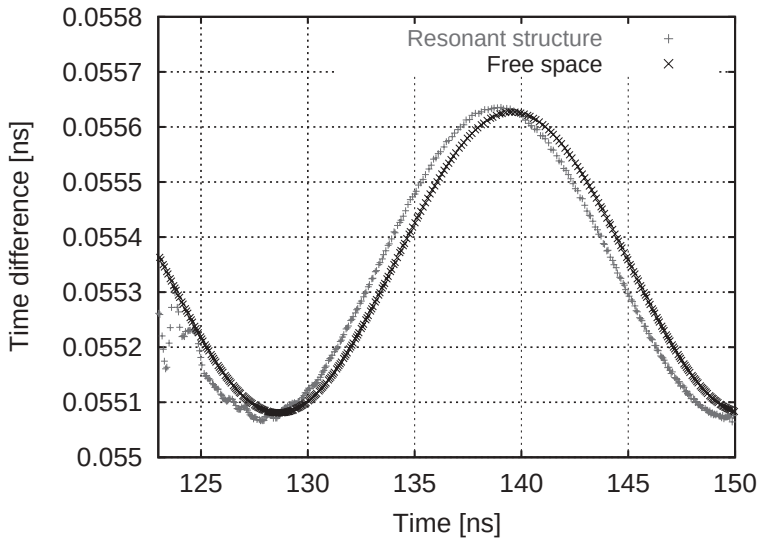

Fig. 18. Calculated frontpart of the FM modulation ($\nu_s = 46$ MHz) of an airborne signal ($\times$) and of a tunneled signal ($+$) front. The tunneled signal, i.e. the modulation is about 0.7 ns faster than the airborne signal. The barrier length was 279.4 mm.

the zeros of the oscillations represents the information. A computer simulation of the time advance of the demodulated signal of a tunneled FM carrier is presented in Fig. 18. The frequency components of the information of the tunneled signal traveled faster than light. The frequency distribution is at the input the same as at the output which is opposite to Winful's incorrect statement [61]. The output frequencies of the signal are connected by causal propagation to the input frequency components. The reason that a superluminal signal does not violate causality is explained below.

Does the measured superluminal signal velocity violate the principle of causality? The line of arguments showing how to manipulate the past in the case of superluminal signal velocities is illustrated in Fig. 19. There are displayed two frames of reference. In the first one at the time $t = 0$ lottery numbers are presented as points on the time coordinate without duration. At $t = -0.5$ s the counters are closed. Mary (A) sends the lottery numbers to her friend Susan (B) with a signal velocity of $4c$. Susan, moving in the second inertial system at a relative speed of $0.75c$, sends the numbers back at a speed of $2c$, to arrive in the first system at $t = -1$ s, thus in time to deliver the correct lottery numbers before the counters close at $t = -0.5$ s.

The time shift of a point on the time axis of reference system A into the past is given by the relation [7,34],

$$t_A = -\frac{L}{c} \cdot \frac{(v_r - c^2/v_s - c^2/v'_s + c^2 v_r/v_s v'_s)}{(c - c v_r/v'_s)}, \tag{22}$$

where L is the transmission length of the signal, v_r is the velocity between the two inertial systems A and B. The condition for the change of chronological order is $t_A < 0$, the time shift between the systems A and B. This interpretation assumes, however, a signal to be a point in the time dimension neglecting its temporal width.

Several experiments are presented above which have revealed superluminal signal velocity in tunneling photonic barriers. Nevertheless, the principle of causality has not been violated as will be explained in the following.

In the example with the lottery data, the signal was assumed to be a point in space–time. However, a physical signal has a finite duration like the pulses sketched along the time axis in Fig. 20.

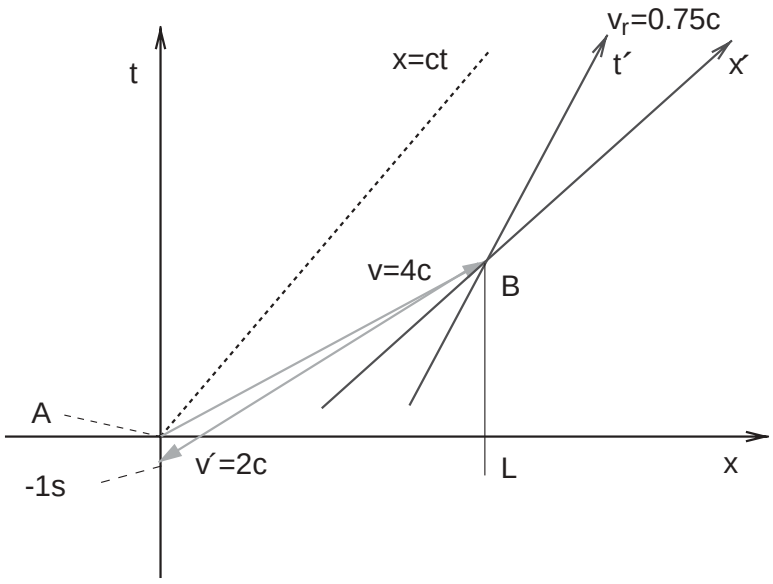

Fig. 19. Coordinates of two inertial observers **A** $(0,0)$ and **B** with $O(x,t)$ and $O'(x',t')$ moving with a relative velocity of $0.75c$. The distance L between **A** and **B** is 2 000 000 km. **A** makes use of a signal velocity $v_s = 4c$ and **B** makes use of $v'_s = 2c$ (in the sketch is $v \equiv v_s$). The numbers in the example are chosen arbitrarily. The signal returns -1 s in the past in **A**.

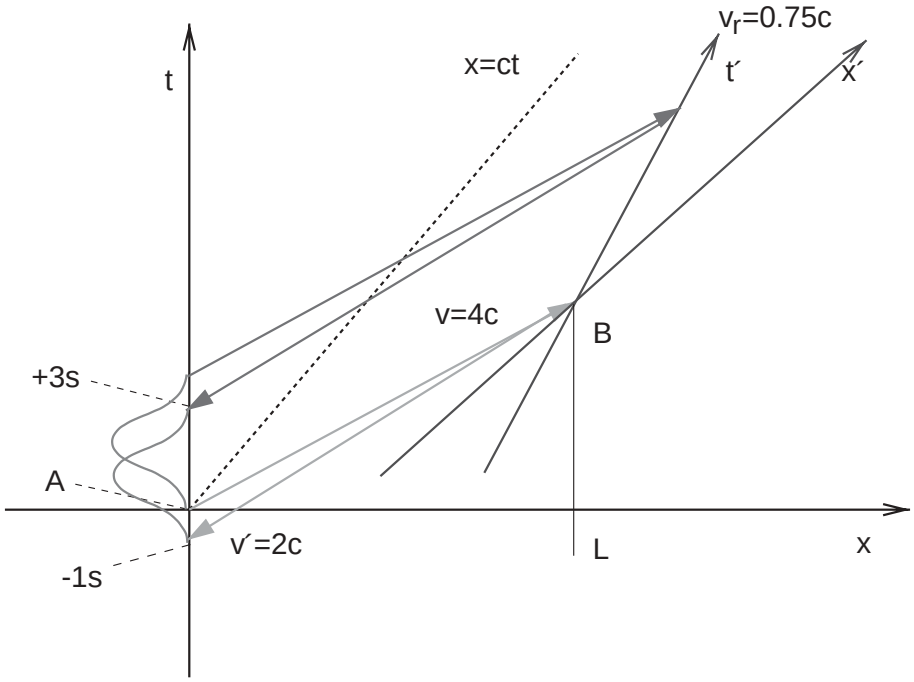

Fig. 20. In contrast to Fig. 19 the pulse-like signal has now a finite duration of 4 s. This data is used for a clear demonstration of the effect. In all superluminal experiments, the signal length is long compared with the measured negative time shift. In this sketch the signal envelope ends in the future with 3 s (in the sketch is $v \equiv v_s$).

The general relationship for the bandwidth–time interval product of a pulse of oscillations is given by

$$\Delta v\, \Delta t \geqslant 1, \tag{23}$$

where Δv is the frequency band of the signal and Δt is the signal duration. A zero time duration of a signal would require an infinite frequency bandwidth.

The maximal amount of information I which can be transmitted over a given signal guide (channel) was determined by Shannon and is discussed in Ref. [62]. It is given by

$$I = \tfrac{1}{3} B_c t_c \log_2(1 + \mathrm{SN}), \tag{24}$$

where B_c is the bandwidth of the channel, t_c is the transmission time (in s), and SN denotes the signal-to-noise ratio (in dB). I is given in bits. The product of frequency band and time duration determines the amount of information of a signal.

Taking into consideration the dispersion relationships of tunneling barriers and other media with a regime of a refractive index which allows superluminal group velocities, the frequency band of a signal has to be narrow in order to avoid nonsuperluminal frequency components and a pulse reshaping.

Assuming a signal duration of 4 s the complete information is obtained with superluminal signal velocity at 3 s in positive time as illustrated in Fig. 20. The compulsory finite duration of all signals is the reason that a superluminal velocity does not violate the principle of causality. A shorter signal with the same

information content would have an equivalently broader frequency bandwidth (Eq. (24)). That means an increase of v_s or v_s' cannot violate the principle of causality.

For instance, the dispersion relation of FTIR (Eq. (8)) elucidates this universal behavior: assuming a wavelength $\lambda_0 = c/v$, a tunneling time $\tau = T = 1/v$, and a tunneling gap between the prisms $d = n \cdot \lambda_0$ $(n = 1, 2, 3, \ldots)$ the superluminal signal velocity is $v_s = n \cdot c$, (remember the tunneling time is independent of barrier length). However, with increasing v_s the bandwidth Δv (that is the tolerated wave number width $\Delta\kappa$) of the signal decreases $\propto 1/d$ in order to guarantee the same amplitude distribution of all frequency components of the signal. In spite of an increasing superluminal signal velocity $v_s \to \infty$ the general causality cannot be violated because the signal time duration increases analogously $\Delta t \to \infty$ (Eq. (24)).

On the other hand assuming a hypothetical signal without a finite time duration, as done in many text books, would lead to an infinite frequency band and infinite energy [16].

6. Universal tunneling time

Theoretical studies, for instance Refs. [2,18,63], and an analysis of several experimental tunneling time data obtained with opaque barriers (i.e. $\kappa \cdot x > 1$) point to a universal behavior [64]. The relations

$$\tau \approx 1/v = T, \tag{25}$$

$$\tau \approx h/W, \tag{26}$$

were found independent of frequency and of the type of barrier studied [64,65]. Here τ, v and T are the tunneling time, the carrier frequency or a wave packet energy W divided by the Planck constant h and the oscillation time of the wave, respectively. The microwave experiments near 10 GHz displayed a tunneling time of about 100 ps and for instance experiments in the optical frequency regime near 427 THz displayed a tunneling time of 2.2 fs. In the case of tunneling forbidden frequency bands of photonic lattices, relationship (25) holds for $n_1/n_2 - 1 \approx 1$, where n_1, n_2 are the refractive indices of the two components of the lattice. The tunneling time of photonic lattices with $n_1/n_2 \approx 1$ becomes much longer than the value given by Eq. (25) as discussed in Section 7.1.

In Ref. [64] it was conjectured that the relation holds also for wave packets with a rest mass having in mind the mathematical analogy between the Helmholtz and the Schrödinger equations. Quantum mechanical studies point to this conjecture [27,33,31,66,67]. Recently, electron tunneling times were measured in a field emission experiment (FEM) [68]. The measured tunneling times are between 6 and 8 fs. Assuming an electron energy of 0.6 eV (the barrier height was 1.7 eV) the empirical relation Eq. (26) yields a tunneling time of 7 fs. Tunneling time data of various experiments are displayed in Table 1 [64]. Some theoretical studies conjectured a universal tunneling time before experimental data were available, for instance Refs. [18,63].

Table 1
Experimental data of the tunneling time and of the reciprocal carrier frequency [64]. The values are measured with different photonic barriers and in different frequency regimes. In the last line electronic data are presented from a field electron microscopic study

Photonic barrier	Reference	Tunneling time τ	Reciprocal frequency $T = 1/v$
FTIR at the	Haibel/Nimtz	117 ps	120 ps
Double-prism	Carey et al.	≈ 1 ps	3 ps
	Balcou/Dutriaux	40 fs	11.3 fs
	Mugnai et al.	134 ps	100 ps
Photonic lattice	Steinberg et al.	2.13 fs	2.3 fs
	Spielmann et al.	2.7 fs	2.7 fs
	Nimtz et al.	81 ps	115 ps
Undersized waveguide	Enders/Nimtz	130 ps	115 ps
FEM	Sekatskii/Letokhov	6–8 fs	> 2.43 fs

7. Superluminal photonic applications

For some applications of the tunneling process there may be two essential restrictions. Tunneling transmission has an exponential attenuation with barrier length. The transmission loss is due to reflection. Actually, the transmission loss is not converted into heat and may be recycled in a special circuit design. The other property which may hamper an application is the tunneling dispersion. Dispersion restricts the application of superluminal tunneling to narrow frequency bands in order to avoid signal re-shaping and nontunneling frequency components. However, there are many technical challenges which do not need a broad frequency band.

7.1. Tunneling

(a) Recently, Longhi et al. [49] performed tunneling of narrow band infrared pulses over a distance of 20 000 wavelengths using a heterostructure of 80 000 quarter wavelength layers. The refractive index of the fiber is $n_1 \approx 1.4$. Experimental results are presented in Fig. 10. The overall distance of the photonic fiber lattice was 20 mm. (Scaling the barrier length to 10 GHz microwaves, the barrier would be 400 m long). The periodic variation of the refractive index along the fiber between the two different quarter wavelength layers is only of the order of 10^{-4}. The measured group (signal) velocity was $2c$ at a transmission intensity of the barrier of 1.5%.

(b) A higher signal speedup to $4.3c$ was obtained in the same infrared frequency regime with a double barrier setup of total length up to 63 mm, by Longhi et al. [43,69]. The arrangement for the 1.5 μm pulse tunneling was similar to that in the sketch of Fig. 5. The measured tunneling time as a function of double barrier distance is presented in Fig. 21. The tunneling time is not constant, but slightly increases with barrier distance as seen from the calculated data in Fig. 21. The

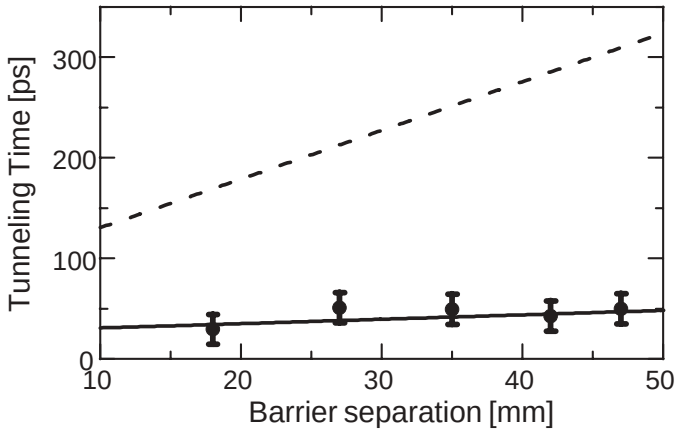

Fig. 21. Tunneling time in an infrared double barrier setup. Data of experimental and calculated (solid line) tunneling time are displayed [43]. The broken line presents the vacuum time.

second term of the tunneling time relation given in Ref. [43] describes the increase. In consequence of this behavior the superluminal group velocity does not increase in proportion to the barrier separation. This result is in agreement with experiments and with the calculations by Longhi [43][3] and by Vetter [70], but it is not in agreement with the calculation by Olkhovsky et al., by Esposito, and by Aharanov [18,44,71]. The discrepancy found between these theoretical calculations depends on the above-mentioned validity of the universal tunneling time of photonic lattice structures. Only photonic lattices with a tunneling time given by Eq. (25) shows a linear dependence of group velocity on barrier length [49,70]. For photonic lattices with a very small periodic change of the refractive index the tunneling time is much larger and an additional term becomes important, with the time τ_2,

$$\tau_2 = T^{1/2} n_0 L/c \tag{27}$$

where T is the reflection intensity and L the distance between the two barriers, determining the group velocity. The long tunneling time and its slight increase with barrier length are seen in Fig. 21.

7.2. Partial reflection by photonic barriers

(a) Photonic barrier reflection is used at 1.5 μm wavelength in fiber optics. Barriers are performed by a 20 mm long piece of glass fiber with a weakly periodically changed refractive index similar to the barrier used in the superluminal transmission experiment by Longhi et al. [49] mentioned above. The losses of reflection by a photonic barrier (purely imaginary impedance) are less than that of a metal due to free carrier absorption. This results in a higher Q-value for a photonic cavity. Photonic barriers represent more effective mirrors than metallic ones. For example

[3] In the paper [43] two wrong numbers are given. The correct values are $\omega_B = 1.216 \times 10^{15}$ and $V_0 = 3.1 \times 10^{-5}$, (Longhi, private communication).

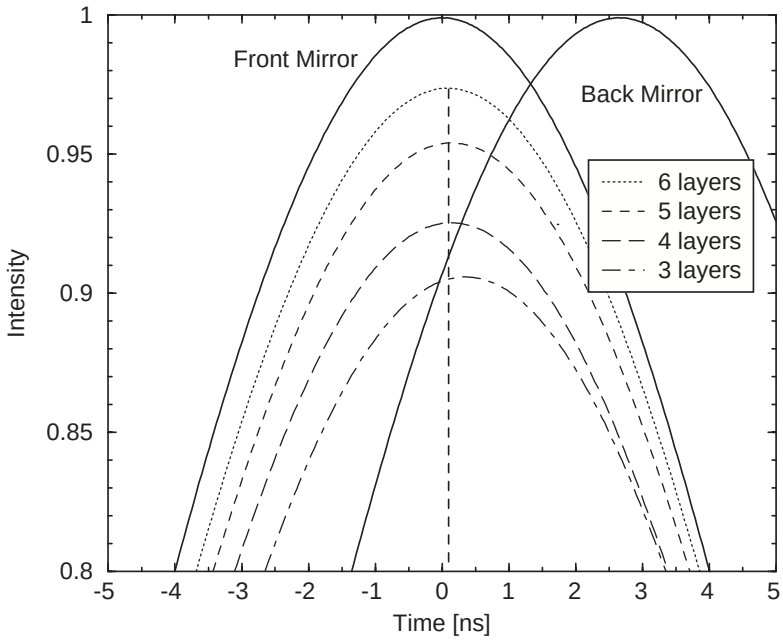

Fig. 22. Measured partially reflected microwave pulses vs. time for varying barrier composition as shown in Fig. 13. The signal reflections from metal mirrors substituting either front or back position of the barrier are displayed. In this example the wavelength was 32.8 mm and the effective barrier length was 410 mm [37].

photonic barriers are profitably used to stabilize infrared laser diodes in optoelectronics.

(b) Fig. 22 shows time-dependent reflection data for two mirrors at different positions. For comparison two photonic barriers were placed at the same positions later. The length of the barriers was varied: by doing so only the magnitude of the reflected pulses was changed, but not the reflection time. The measured reflection time of about 100 ps equals the universal tunneling time observed in transmission of the barrier. The nonlocal behavior of tunneling modes gives the information on barrier length at the barrier front within one oscillation time of the signal [37]. An ultrafast modulator was designed on the basis of partial reflection [72]. The effective barrier length is modulated by an electric field induced change of the refractive index at half of the total barrier length. This results in an amplitude change of reflection within the tunneling time, see Fig. 22.

Another type of modulation can be achieved due to a local change of refractive index by signals exciting an optically active dielectric medium. For example this principle has been applied in experiments on negative group velocity, see e.g. Ref. [22]. In the case of the above microwave experiment the modulations at the distance of 150 mm away from the barrier entrance appears at the barrier front within 100 ps, whereas the corresponding luminal propagation time is five times longer.

7.3. Partial reflection by asymmetric photonic barriers

An interesting property of asymmetric photonic barriers has been studied recently by Longhi [73]. Assuming the one-dimensional barrier to differ in scattering

potential at its two sides, he calculated the reflection times τ_{r+} and τ_{r-} of a wave group by each barrier side, respectively. He obtained the following relationship between the time τ and the two reflection times:

$$\tau = \tau_{r+} + \tau_{r-}. \tag{28}$$

In Ref. [73], the tunneling or traversal time τ is called transition time τ_t. The amazing result of the calculation is that in the case of asymmetric barriers one reflection time may be positive, whereas the other one becomes negative. The theoretical data shown in Fig. 23 were calculated assuming a standard fiber as used in optoelectronics. The asymmetric fiber Bragg grating barrier has a narrow transmission window as shown in Fig. 23(a). The author suggested an experimental verification of the theoretical data.

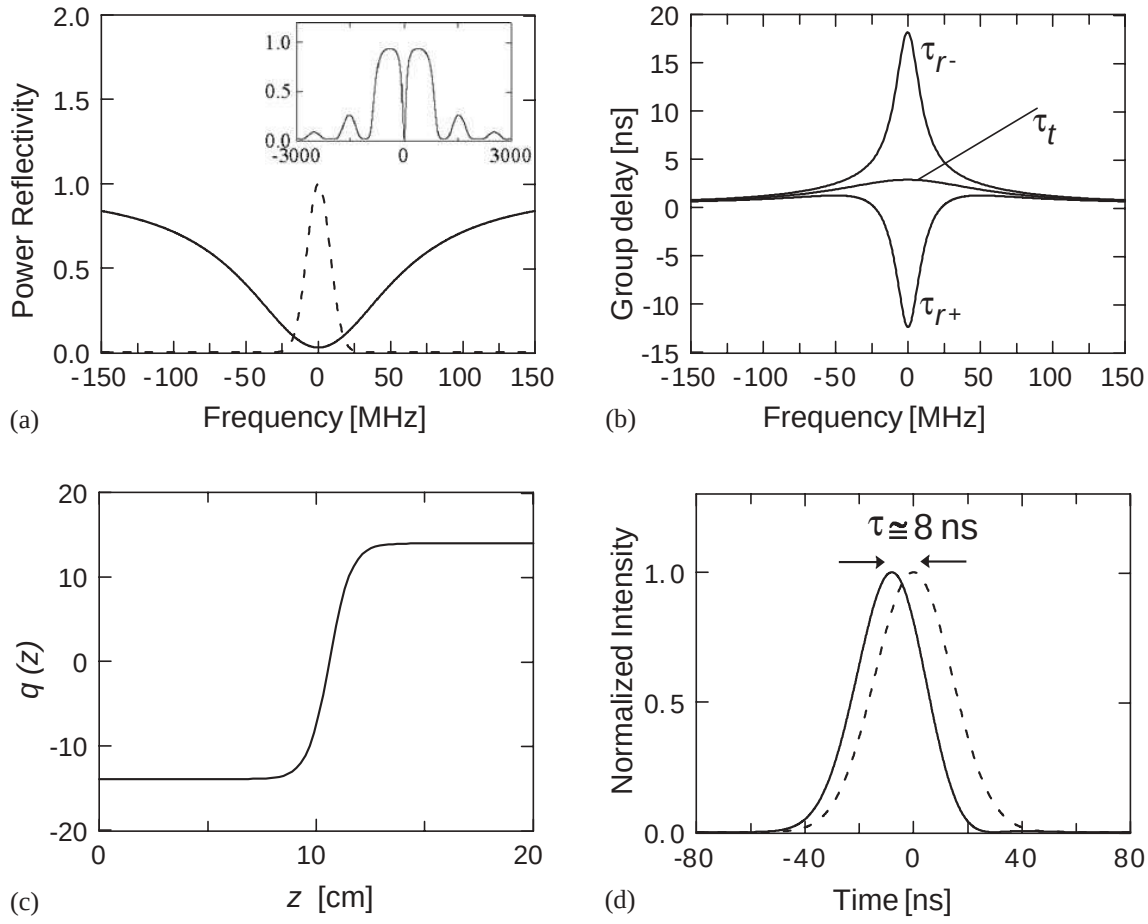

Fig. 23. Calculated partial reflection by an asymmetric barrier at a wavelength of 1.5 μm [73]. (a) Spectral reflectivity around the reflection minimum of the transmission window of an asymmetric photonic barrier. The broken line represents the spectrum of the incident pulse. (b) Group delay times. (c) Scattering potential $q(z)$ for a uniform fiber Bragg grating with a π phase jump in the center. Barrier length 200 mm, average refractive index of the fiber Bragg grating is $n = 1.5$. (d) The peak of the reflected pulse leaves the grating at the input plane 8 ns before the incident peak entered into the grating. The peak pulse advancement on the fiber corresponds to a distance of 1.6 m in the fiber or 2.4 m in vacuum.

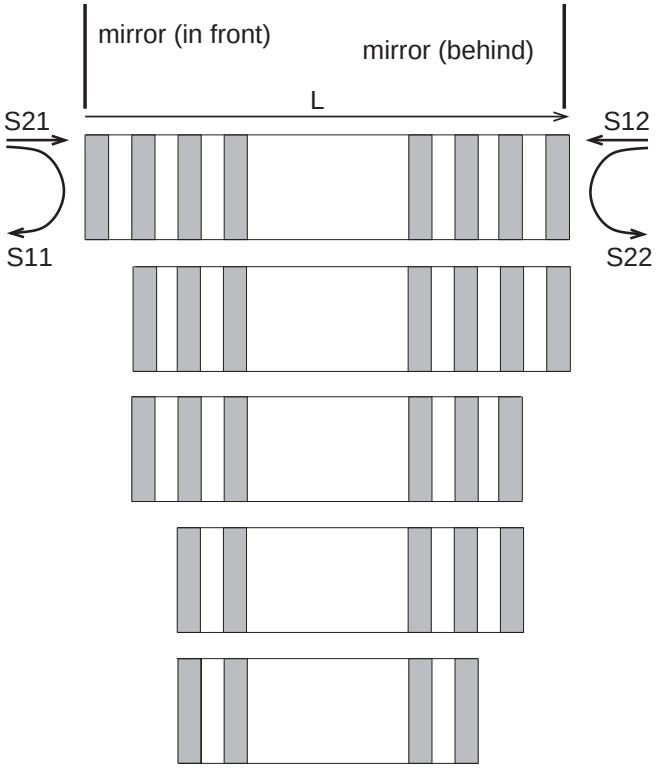

Fig. 24. Sketch of the resonant quarter wavelength structure. The structure was shortened beginning with 8 by one slab of perspex down to only one slab after each measurement.

Quite recently Ref. [74] microwave experiments were carried out which confirmed these predictions. The experimental procedure is displayed in Fig. 24. Here S_{11}, S_{12}, S_{21}, S_{22} are the scattering matrix elements describing reflection and transmission, respectively. The predicted effect of an asymmetric reflection time was measured near the forbidden frequency gap ($\approx$7–10.5 GHz) of the photonic lattice at a transmission window at a frequency of 11.85 GHz. The measured transmission time at 11.85 GHz was subluminal, whereas the phase and thus the reflection time showed superluminal behavior in agreement with Eq. (28) for the asymmetric barrier arrangement. The data is displayed in Figs. 25 and 26. The group reflection time oscillates around the subluminal transmission time. Reflection times below ≈ -100 ps are resulting in a superluminal group velocity. The asymmetric barrier represents a novel device for the realization of sub- and superluminal group reflection times.

8. Electronic applications

8.1. The tunneling diode

The first man-made tunneling device was the semiconductor tunneling diode. It was invented by Esaki around 1960 [75]. This nonlinear electronic device has still a

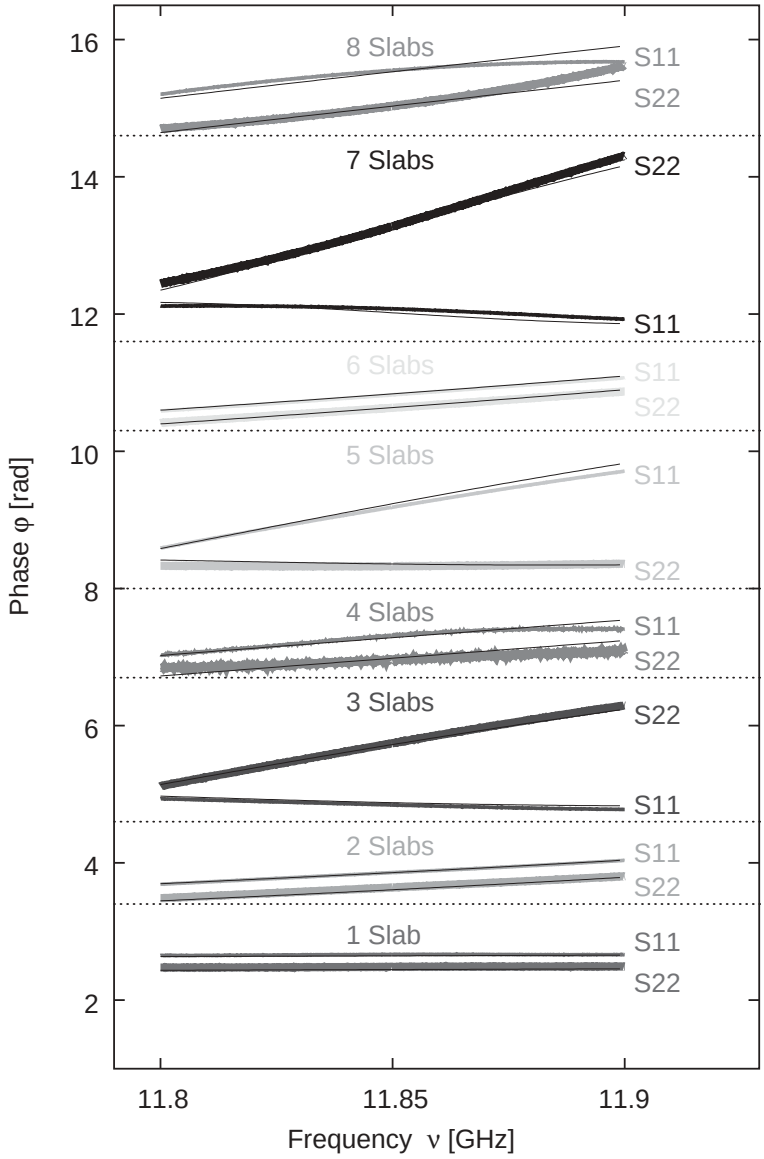

Fig. 25. Measured partial reflected phase shift vs. frequency by an asymmetric barrier of different of slab arrangements. The phase behavior is identical in both direction in the symmetrical cases but differs in the asymmetric cases.

growing market. However, the tunneling time which would give the ultimate dynamical specification of such a diode has never been measured yet. Our conjecture is: the universal photonic tunneling time Ref. [64] is valid also for the electronic tunneling process. Actually, recent electronic tunneling-time experiments support this conjecture [68]. The experimental data is in agreement with relation (26).

The tunneling time of the Esaki diode has not been determined so far. The measured diode response time is covered by parasitic effects like the much longer interaction time of electrons with chemical impurities and structural lattice defects present in a semiconductor.

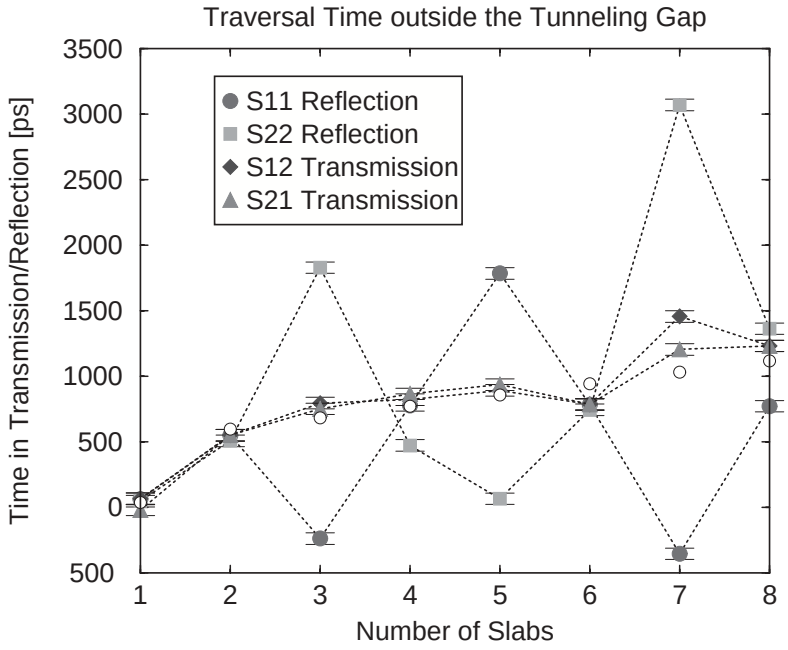

Fig. 26. Measured transmission and reflection time vs. number of slabs of the barrier structure outside the forbidden frequency gap at a frequency of 11.85 GHz. The reflection times oscillate around the transmission time in the asymmetric arrangement of the barrier.

Electronic resonant tunneling was studied in III–V semiconductor quantum wells [76]. The experiments gave information on the dynamical behavior of the various double barrier structures. However, the determined time response in the case of resonant tunneling is determined by the resonator quality (the resonance line width) and not by the tunneling time. The tunneling time is several orders of magnitude shorter than the resonator lifetime as was shown in a photonic analogy experiment [77].

8.2. *Superluminal electron transport*

It was shown in several quantum mechanical studies, for instance by Low and Mende that *a particle suitably localized in space and time*, *which is transmitted through a long*, *high barrier*, *travels as if it tunneled it in zero time* [31]. Of course, the time spent inside the barrier only was considered. Again as in the case of photonic tunneling the barrier traversal velocity was superluminal even in the case of relativistic analyses [31,33,66,67].

Electronic transport in a semiconductor is rather slow compared with the velocity of light. The highest electron velocity is achieved in the ballistic electron transport as in the case of an electron microscope or some special semiconductor nano-device structures. Bias voltages of electronic devices are of the order of 1V. The voltage results in a ballistic electron velocity of the order of 10^6 m/s, which is two orders of magnitude smaller than c.

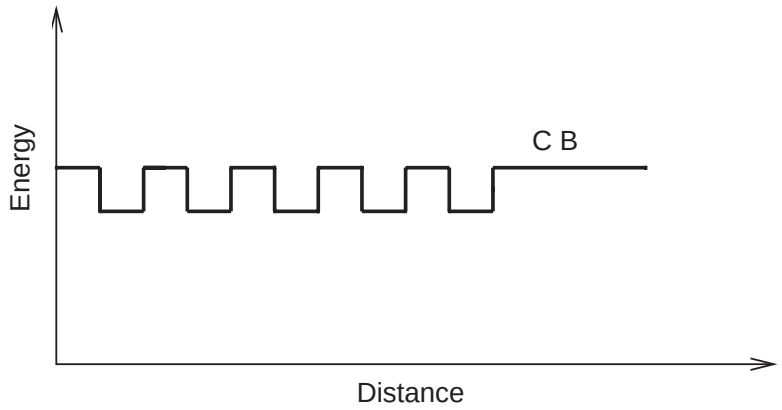

Fig. 27. Sketch of the conduction band edge (CB) of Si periodically doped with Si and SiGe at quarter wavelength distances. The SiGe alloy has a smaller band gap than Si [78].

8.2.1. Electronic lattice structures

We propose an electronic lattice structure with alternating quarter wavelength layers of slightly different band gaps, which can be traversed at superluminal speeds. This is in analogy with the photonic lattice structure of Fig. 10. The conduction band electron wavelength is of the order of 1 nm. Ultrafast coupling of electronic device elements in a circuit could be performed and accelerate the speed of computers. For instance a periodic structure of Si/SiGe quarter wavelength layers represents an electronic lattice. Such a doping of a Si-semiconductor structure with the SiGe alloy yields a weak variation of the band gap as sketched in Fig. 27 which is analogous to the periodic dielectric fiber structure mentioned above [49].

Such electronic structures may exceed lengths of more than 1 μm and could be used to perform ultra-fast interconnections between device elements.

8.2.2. pn-Tunnel junctions

Interband tunneling, the basis of the classical tunneling diode, can also be used for fast electronic interconnections. By an appropriate doping profile the tunneling path can be adjusted between some hundred nanometres to several thousand nanometres.

There is a problem remaining for all tunneling applications: the high reflection at the barrier entrance. However, tunneling is not a dissipative process, there is no energy loss. As mentioned above the reflected electronic power should be recycled by a smart circuit design.

9. Summary

Photonic tunneling is traceable through barriers of thousands of wavelengths; the photons do not spend time inside the barrier. The latter is an experimental result due to the fact that the transmission and the reflection time is independent of the barrier length in agreement with quantum mechanical calculations (Hartman effect [27,28,79,29]). Another proof of the zero-time behavior of a barrier is observed in

the case of the symmetrical double prisms setup for FTIR, where the reflected and the transmitted signal are shown to have the same delay time [39]. Thus the time spent inside the barrier or in the double prism gap is zero. The measured finite transmission time comes into existence at the entrance boundary of the photonic barriers. As experiments have demonstrated, tunneling is realized by nonlocal fields and is represented by virtual photons [18,37,40,80]. However, the principle of causality has not been violated by superluminal signals as a result of the finite signal duration and the corresponding finite frequency bandwidth. But, amazingly enough, the time span between cause and effect is reduced by a superluminal signal velocity compared with the time span in the case of light propagation from cause to effect in vacuum.

The tunneling process shows strange properties in the case of opaque barriers, unfamiliar from classical physics. The tunneling time is universal and arises at the barrier front. It equals approximately the reciprocal frequency of the carrier frequency or of the wave packet energy divided by the Planck constant h.

Another strange aspect of the phenomenon is that evanescent fields are solutions of the Maxwell equations, but they are not fully describable by them. They carry a *negative* energy which makes it impossible to detect them [12,38,81] and they are nonlocal. Incidentally, their properties are in agreement with wave mechanical tunneling.

The energy of signals is always finite, resulting in a limited frequency spectrum [17]. This is a consequence of Planck's quantization of radiation, with an energy minimum of $\hbar\omega$ for radiation of angular frequency ω. An electric field cannot be measured directly. Detectors need at least one energy quantum $\hbar\omega$ in order to respond. This is a fundamental deficiency of classical physics, which assumes any small amount of field and charge is measurable.

The front and the end of a frequency band limited signal are continuous in time rather than discontinuous, as for an ideal signal [5,25]. The latter would need infinitely high frequency components. Furthermore, signals are not represented by analytic functions, otherwise the complete information would be contained in the forward tail of the signal [55].

According to Collins et al. [33], the disputes on zero tunneling time (the time spent inside a barrier) become redundant after reading the papers by Wigner and by Hartman. The discussions about superluminal tunneling remind us of the problem of multiplex transmission displayed in Fig. 4. Here the finite time duration and frequency band limitation of a signal violate causality according to Fourier transforms. However, no one has heard a phone ring before the sendering phone was switched on. This indicates the crucial role of finite frequency bands and finite time duration of physical signals, without violating the principle of causality [17].

Irrespective of the argument about violation of Einstein causality, all the properties introduced above will surely prove useful for novel fast devices, for the field of photonics and also the field of electronics.

Acknowledgements

I gratefully acknowledge the encouragement by Professor P.T. Landsberg to write this second article on Superluminal Tunneling and the elucidating discussions on this topic with T. Bracken, A. Haibel, A. Stahlhofen, and R.-M. Vetter.

References

[1] G. Nimtz, W. Heitmann, Progr. Quantum Electron. 21 (1997) 81.
[2] E. Recami, Int. J. Mod. Phys. A 15 (2000) 2793.
[3] A. Sommerfeld, Vorlesungen über Theoretische Physik, Band IV, Optik Dieterich'sche Verlagsbuchhandlung, 1950.
[4] R.P. Feynman, Lectures on Phys. II, 1964, 33–12.
[5] L. Brillouin, Wave Propagation and Group Velocity, Academic Press, New York, 1960.
[6] R. Chiao, A. Steinberg, Progr. Opt. XXXVII (1997) 345.
[7] R. Sexl, H. Schmidt, Raum-Zeit-Relativität, Vieweg Studium, Braunschweig, 1978.
[8] R.U. Sexl, H.K. Urbantke, Relativity, Groups, Particles, Springer, Wien, New York, 2001.
[9] M. Fayngold, Special Relativity and Motions Faster than Light, Wiley-VCH, Weinheim, 2002, pp. 219–223.
[10] J.D. Jackson, Classical Electrodynamics, 3rd Edition, Wiley, New York, 1998, p. 326.
[11] A. Einstein, Ann. Phys. (Leipzig) 17 (1905) 891.
[12] G. Nimtz, Gen. Relativity Gravitation 31 (1999) 737.
[13] E. Merzbacher, Quantum Mechanics, 2nd Edition, Wiley, New York, 1970.
[14] The IEEE Standard Dictionary of Electrical and Electronics Terms, IEEE Standard no.: 100-1996.
[15] G. Nimtz, Ann. Phys. (Leipzig) 7 (1998) 618.
[16] G. Nimtz, Eur. Phys. J. B 7 (1999) 523.
[17] G. Nimtz, A. Haibel, Ann. Phys. (Leipzig) 11 (2002) 163.
[18] V. Olkhovsky, E. Recami, Phys. Rep. 214 (1992) 339;
V. Olkhovsky, Consiglio Nazionale delle Ricerche, Roma, Monografie Scientifiche, Serie Scienze Fisiche, 2001, International Conference, Napoli, October 3–5, 2000, in: D. Mugnani, A. Ranfagni, L. Schulman (Eds.), Time's Arrows, Quantum Measurement and Superluminal Behavior, Istituto Italiano per gli Studi Filosofici, Napoli. p. 173.
[19] H.M. Brodowsky, W. Heitmann, G. Nimtz, Phys. Lett. A 222 (1996) 125.
[20] A.P.L. Barbero, H.E. Hernandes-Figueroa, E. Recami, Phys. Rev. E 62 (2000) 8628.
[21] B. Segard, B. Macke, Phys. Lett. 109A (1985) 213.
[22] L. Wang, A. Kuzmich, A. Dogariu, Nature 406 (2000) 277.
[23] R.W. Ziolkowski, Phys. Rev. E 63 (2001) 046604.
[24] E. Recami, Riv. N. Cim. 9 (1986) 1.
[25] A. Papoulis, The Fourier Integral and its Applications, McGraw-Hill, New York, 1962, Sections 7.5 and 7.6.
[26] NTIA 2000, National Telecommunication and Information Administration (USA), American National Standard of Telecommunication Terms.
[27] Th. Hartman, J. Appl. Phys. 33 (1962) 3427.
[28] A. Enders, G. Nimtz, Phys. Rev. E 48 (1994) 632.
[29] Ch. Spielmann, R. Szipöcs, A. Stingl, F. Krausz, Phys. Rev. Lett. 73 (1994) 2308.
[30] F.S. Crawford, Berkeley Physics Course, Vol. 3, Waves, McGraw-Hill Book Company, Inc., New York, London, 1968 (Chapter 6).
[31] F.E. Low, P.F. Mende, Ann. Phys. NY 210 (1991) 380.
[32] R. Landauer, Th. Martin, Rev. Mod. Phys. 66 (1994) 217.
[33] S. Collins, D. Lowe, J. Barker, J. Phys. C 20 (1987) 6213.
[34] P. Mittelstaedt, Eur. Phys. J. B 13 (2000) 353.

[35] H.D. Lüke, IEEE Commun. Magazine April (1999) 106–108.
[36] C.E. Shannon, Bell Sys. Tech. J. 27 (1948) 379, 623;
C.E. Shannon, Proc. IRE 37 (1949) 10.
[37] G. Nimtz, A. Haibel, R.-M. Vetter, Phys. Rev. E 66 (2002) 037602.
[38] O. Bryngdahl, Progr. Opt. 11 (1973) 167.
[39] A. Haibel, G. Nimtz, A.A. Stahlhofen, Phys. Rev. E 63 (2001) 047601.
[40] C.K. Carniglia, L. Mandel, Phys. Rev. D 3 (1971) 280;
C.K. Carniglia, L. Mandel, J. Opt. Soc. Am. 61 (1971) 1035.
[41] A. Enders, G. Nimtz, J. Phys. I France 2 (1992) 1693;
A. Enders, G. Nimtz, J. Phys. I (France) 3 (1993) 1089.
[42] V. Olkhovsky, E. Recami, G. Salesi, Europhys. Lett. 57 (2002) 879.
[43] S. Longhi, P. Laporta, M. Belmonte, E. Recami, Phys. Rev. E 65 (2002) 046610.
[44] S. Esposito, Phys. Rev. E 67 (2003) 016609.
[45] Ph. Balcou, L. Dutriaux, Phys. Rev. Lett. 78 (1997) 851.
[46] J.J. Carey, J. Zawadzka, A. Jaroszynski, K. Wynne, Phys. Rev. Lett. 84 (2000) 1431.
[47] A.A. Stahlhofen, Phys. Rev. A 62 (2000) 12112.
[48] J.J. Hupert, Appl. Phys. 6 (1975) 131.
[49] S. Longhi, M. Marano, P. Laporta, M. Belmonte, Phys. Rev. E 64 (2001) 055602.
[50] J.A. Stratton, Electromagnetic Theory, McGraw-Hill Book Company, Inc., New York, London, 1941.
[51] A. Steinberg, P. Kwiat, R. Chiao, Phys. Rev. Lett. 71 (1993) 708.
[52] A. Steinberg, P. Kwiat, R. Chiao, Phys. Rev. Lett. 68 (1992) 2421.
[53] E. Desurvivre, Sci. Am. 266 (1992) 96.
[54] D. Leeper, Sci. Am. 268 (2002) 46.
[55] F. Low, Ann. Phys. (Leipzig) 7 (1998) 660.
[56] M. Büttiker, H. Thomas, Superlattices Microstruct. 23 (1998) 781.
[57] Hewlett Packard, Spectrum Analysis Application Note 150, 1989.
[58] H. Aichmann, G. Nimtz, H. Spieker, Verhandlungen der Deutschen Physikalischen Gesellschaft 7 (1995) 1258.
[59] Th. Emig, Phys. Rev. E 54 (1996) 5780.
[60] G. Diener, Phys. Lett. A 235 (1997) 118;
H. Goenner, Ann. Phys. (Leipzig) 7 (1998) 774.
[61] H.G. Winful, Phys. Rev. Lett. 90 (2003) 023901.
[62] A.A. Stahlhofen, to be published.
[63] A. Ghatak, S. Banerjee, Appl. Opt. 28 (1989) 1960.
[64] A. Haibel, G. Nimtz, Ann. Phys. (Leipzig) 10 (2001) 707.
[65] S. Esposito, Phys. Rev. E 64 (2001) 026609.
[66] C.R. Leavens, G.C. Aers, Phys. Rev. B 40 (1989) 5387;
C.R. Leavens, W.R. McKinnon, Phys. Lett. A 194 (1994) 12.
[67] J.K. Tomfohr, O.F. Sankey, S. Wang, Phys. Rev. B 66 (2002) 235105.
[68] S.K. Sekatskii, V. S. Letokhov, Phys. Rev. B 64 (2001) 233311.
[69] S. Longhi, M. Marano, P. Laporta, O. Svelto, J. Opt. Soc. Am. B 19 (2002) 2742.
[70] R.-M. Vetter, to be published.
[71] Y. Aharanov, N. Erez, B. Reznik, Phys. Rev. A 65 (2002) 052124-1.
[72] A. Haibel, G. Nimtz, pending, Deutshes Patent - und Markenamt. No. 101 16 946.9-35 (28.03.2002).
[73] S. Longhi, Phys. Rev. E 64 (2001) 037601-1.
[74] A. Haibel, R.-M. Vetter, G. Nimtz, to be published.
[75] L. Esaki, IEEE Trans. ED-23 (1976) 644.
[76] T. Sollner, W. Goodhue, P. Tannewald, C. Parker, D. Peck, Appl. Phys. Lett. 43 (1983) 588;
W. Goodhue, T. Sollner, H. Le, E. Brown, B. Vojak, Appl. Phys. Lett. 49 (1986) 1086;
T. Sollner, E. Brown, W. Goodhue, H. Le, Appl. Phys. Lett. 50 (1986) 332.
[77] G. Nimtz, H. Spieker, A. Enders, J. Phys. I France 4 (1994) 565.
[78] S.M. Sze, Physics of Semiconductor Devices, 2nd Edition, Wiley, New York, 1981.

[79] M. Campi, M. Cohen, IEEE Trans. Electron. Dev. ED-17 (1970) 157.
[80] E. Recami, Consiglio Nazionale delle Ricerche Roma, Monografie Scientifiche, Serie Scienze Fisiche, 2001, International Conference, Napoli, October 3–5, 2000, in: D. Mugnani, A. Ranfagni, L. Schulman (Eds.), Time's Arrows, Quantum Measurement and Superluminal Behavior, Istituto Italiano per gli Studi Filosofici, Napoli. p. 17.
[81] S. Gasiorowicz, Quantum Physics, 2nd Edition, Wiley, New York, 1996.